Shock wave formation in a dc glow discharge dusty plasma

V. E. Fortov, O. F. Petrov, V. I. Molotkov,* M. Y. Poustylnik, V. M. Torchinsky, V. N. Naumkin, and A. G. Khrapak
Institute for High Energy Densities, Russian Academy of Sciences, Izhorskaya 13/19, Moscow 125412, Russia
(Received 7 April 2004; published 28 March 2005)

A jump of dust density propagating through the dusty plasma structure has been observed. To excite the disturbance an impulse of axial magnetic field to the dusty plasma in a dc glow discharge striation has been applied. This impulse resulted in the dynamical stretching of the dusty plasma structure. During the reconstruction of the structure a ramp-shaped perturbation of dust density appeared. The perturbation was steepening and formed into a dust-acoustic shock. The anomalously high shock compression is observed.

DOI: 10.1103/PhysRevE.71.036413 PACS number(s): 52.27.Lw, 52.35.Tc, 52.35.Fp, 52.35.Mw

I. INTRODUCTION

Shock waves, i.e., discontinuous disturbances propagating through different media, are known to exist in plasmas. They arise from large-amplitude perturbations as a result of interplay between the nonlinearity and different dissipation processes. In [1] an observation of an ion-acoustic shock obtained in a Q machine was reported. The shock front thickness in this case was determined by the ion-ion collisions. A collisionless ion-acoustic shock was obtained in a double plasma device [2]. In this case the shock thickness is governed by the Landau damping. In complex (dusty) plasmas the existence of the shock waves was for the first time theoretically predicted in [3]. Further studies of shocks in dusty plasmas are based upon the Korteveg–de Vries–Burgers equation [4] and application of conservation laws to a discontinuous disturbance with consequent derivation of the Hugoniot equation [5]. Experimental attempts to achieve a plane shock in 2D structures are unsuccessful up to the present time [6] since no steepening of large-amplitude compressions was achieved. However, 2D Mach cones which in fact are shock waves with the V-shaped front produced by the supersonic object traveling through the medium were observed [7,8]. Very recently an observation of a shock wave in 3D complex plasma was reported [9]. The experiment was carried out in the rf discharge under the microgravity conditions using the PKE-Nefedov laboratory. A perturbation was excited by a gas pulse from an electromagnetic valve.

In our previous investigations of the dc glow discharge dusty plasma we observed the self-excited dust acoustic waves [10] and recently the dust density waves excited by the gas-dynamic impact [12]. The latter appeared to have quite high amplitude and to be rather steep. However the process of the steepening was not observed. In this work we present an observation of a traveling perturbation produced in a dc glow discharge complex (dusty) plasma. The perturbation was formed after a short electromagnetic impulse and first appeared as ramp-shaped. While traveling the perturbation was observed to steepen and finally it appeared to develop into a dust-acoustic shock.

*Electronic mail: molotkov@ihed.ras.ru

II. EXPERIMENTAL SETUP

The experiment was performed in a vertically positioned glass tube of the inner diameter 3.6 cm and 40 cm interelectrode distance. The tube was filled with neon and the stratified glow discharge with cold electrodes was created inside it. Dust particles were injected into the plasma from a container placed above the discharge area. While levitating in the striations the dust grains were illuminated with a "laser sheet" and the scattered light was registered by a digital videocamera with the frame rate of 1000 frames/s and spatial resolution of 20 μm/pixel. In more details the installation is described elsewhere [13]. For this experiment the tube was filled neon at pressure of 0.5 mbar. Discharge current was adjusted at 4.2 mA. Plastic spherical dust particles 1.87 μm in diameter were injected into the plasma.

To provide the electromagnetic impulse the following scheme was introduced [Fig. 1(a)]. 16 loops of copper wire all in one horizontal plane were coiled around the discharge tube (impulse coil). A battery of high-voltage capacitors with the total capacity of 1.2 mF was charged up to 1.2 kV and then discharged onto the coil through the $R=14\ \Omega$ resistor. The impulse shape was measured with the help of the Rogovsky coil. The schematical impulse profile and its typical parameters are shown in Fig. 1(b). Due to the low inductivity of the impulse coil the rapid ($\sim$0.1 ms) current growth is observed. The current decay is determined by the battery capacitance C and resistance R and lasts about 10 ms. The current impulse amplitude is of the order of 90 A. The corresponding amplitude of the magnetic field inside the coil is estimated to be 150 G.

III. EXPERIMENTAL RESULTS

A. Video observations

The impulse applied affects the striation only and produces no influence on the dust particles because of their high inertia. The striation could be observed by the videocamera as a bright background glow. The initial structure is shown in Fig. 2(a). When the impulse circuit is closed the striation rapidly, i.e., for a time less than the frame duration moves upward towards the anode [glow disappears in Fig. 2(b)]. As the striation moves away the dust particles loose equilibrium and start falling down under the effect of the gravitational

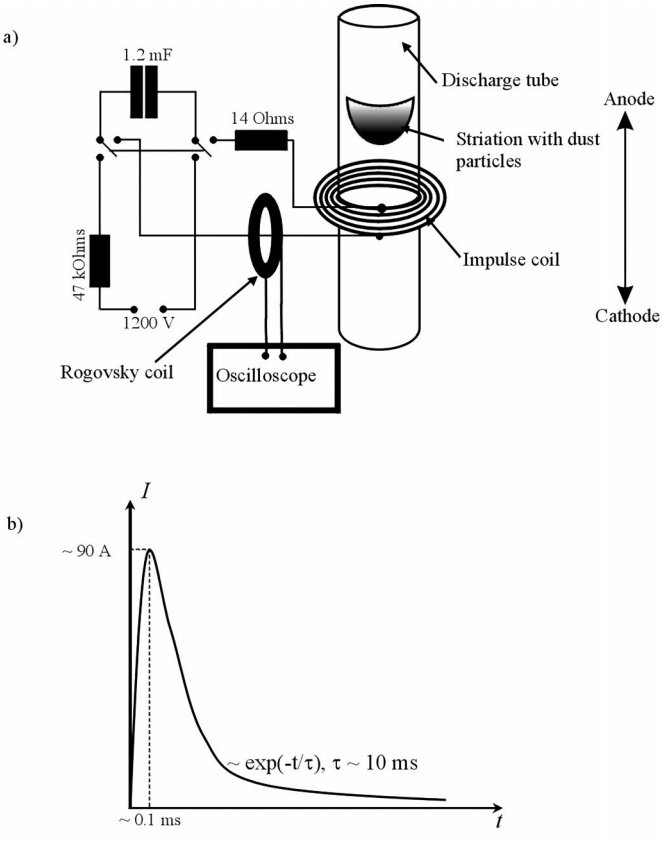

FIG. 1. Scheme of the electromagnetic impulse experiments (a). The impulse shape, registered by the Rogovsky coil, is given schematically in (b).

force [Fig. 2(c)] since the area with the high electric field moves away with the striation. Then as the current is decreasing the striation is moving backwards. The returning striation drags the particles upward [Figs. 2(d) and 2(e)]. Lower particles have more time to fall down than the upper ones. This leads to the "stretching" of the structure [compare Figs. 2(b) and 2(f)]. In the next stage we observe the pronounced division of the structure into two parts with different particle velocities and densities (Fig. 3). Upper particles settle in their initial configuration whereas in the lower part

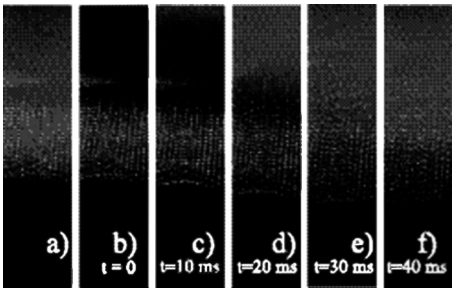

FIG. 2. Sequence of videoimages, presenting the behavior of the dust cloud and the striation under the effect of the magnetic impulse; (a) is the initial structure; $t=0$ corresponds to the electromagnetic impulse launch. The images are adjusted so that the striation is seen as a bright background glow. Size of each image is 5.0 $\times$ 20.5 mm.

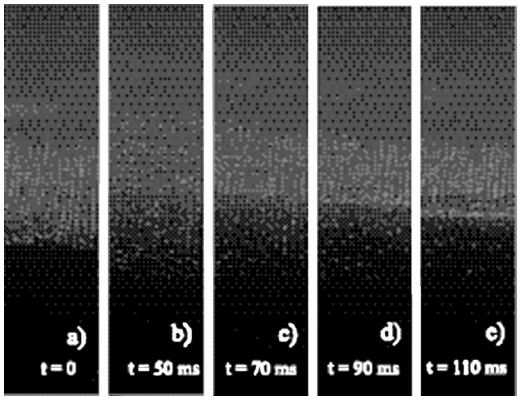

FIG. 3. Sequence of the images, presenting the formation of the discontinuity front. Size of each image is 5.4 $\times$ 20.5 mm.

of the structure the dust density is still reduced and the dust grains inside it are running upward. Therefore the discontinuity in the dust subsystem is formed. In the further development of the situation the front of the discontinuity escapes from the high density part. Such an escape repeats many times, i.e., the perturbation turns into the damping oscillations. Movies of our shock is available on the corresponding web page [11]. In this paper we concentrate on the formation and propagation of the discontinuity.

We should note that our previous experiments with the gas-dynamic influence [12] were also based on the relative displacement of the striation and the dust cloud. In that case the striation was stationary and the impact of the gas flow was dragging the dust particles. The relative velocity of the striation and the dust cloud in that experiment might not exceed the velocity of the gas flow, i.e., 30–40 cm/s. In the present work the electrodynamic impact provides the fast motion of the striation, whereas the dust particles move much slower downward under the effect of the excess gravitational force. The characteristic speed of the striation which in the present situation is the relative speed of the striation and the dust cloud is estimated to be more than 100 cm/s, 2–3 times higher than that in the case of gas-dynamic impact. This explains the significant difference in the behavior of the dust particles in these two experiments.

B. Dust densities

Having particle positions determined with the subpixel resolution [14] for each videoframe we could derive the densities and velocities corresponding to each moment of time. Since our wave performs the one-dimensional motion we treated the distribution of the density along the vertical axis only. The density was determined as follows. First we counted the numbers of the dust particles in the 400 μm thick horizontal stripes of each videoframe. The 3D density was then calculated as this number divided by the product of the stripe area and the illuminating laser sheet thickness. The latter was measured to be 230 μm.

The steepening of the perturbation is obvious in Fig. 4, where the shapes of the dust density versus the vertical coordinate corresponding to the images in Fig. 3, are presented.

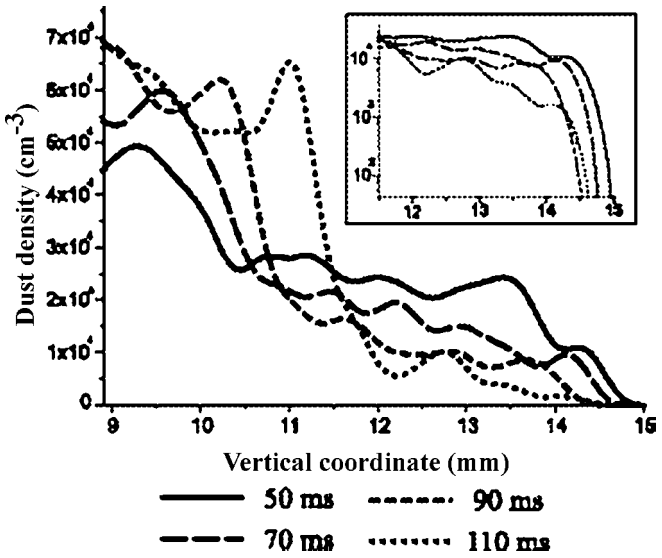

FIG. 4. Spatial profiles of the dust density of the front of the perturbation at different moments of time. The curves indicate pronouced steepening of the perturbation. Low density parts of the perturbation are shown separately in the frame.

As we see the front steepens from 50 ms to 90 ms. At 90 and 110 ms the inclinations of the front are about to be equal, so that we may state that the front of the perturbation becomes stationary. The average velocity of the front after it has become stationary is $V=3.8$ cm/s.

C. Dust velocities and kinetic energies

We have plotted a map of dust particle velocities determined for three consecutive videoframes (Fig. 5). Before the shock front the dust particles are observed to stream upward. This map once again confirms that what we observe is a real discontinuity of dust density and speed.

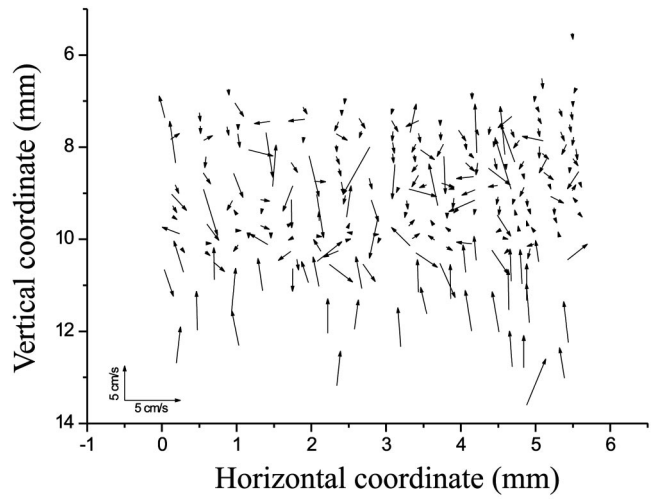

FIG. 5. Map of the dust particle velocities, determined from the particle displacements between $t=70$ ms and $t=72$ ms. The start points of the vectors show the initial particle positions. The length of each vector indicates the magnitude of the velocity according to the given scale.

We also analyzed the distributions of the dust particles over the velocities along the vertical and horizontal axes. To obtain the statistically representative distributions we determined the particle velocities on 30 consecutive videoframes—starting at 90 ms and finishing at 120 ms. The distributions were determined separately for the areas before and behind the front of the perturbation. These distributions are shown in Fig. 6. From these distributions we obtain the drift velocities of the dust particles and their average energies. The average velocity of the dust particles ahead of the front is in the upward direction and equals $U_1=5.1$ cm/s. Behind the front we see a slow drift of dust particles in the downward direction with the average velocity $U_2=0.8$ cm/s. Therefore the speed of the front in the reference system connected with the upstreaming dust particles in the rarefaction $D_1=U_1+V=8.9$ cm/s. With respect to the downstreaming particles in the high density part the front is moving with the velocity $D_2=V-U_2=3.0$ cm/s.

The values of the characteristic kinetic energies obtained from the velocity distributions show that ahead of the front the dust particles are not in the thermal equilibrium since the kinetic energy of the dust particles along the vertical axis is significantly larger than that along the horizontal axis. Behind the front the kinetic energies along both axes are the same if the uncertainties are taken into account. So we may suppose the thermal equilibrium there.

IV. Discussion

The dust density ahead of the shock front is decreasing, it means that the shock is traveling in the nonuniform medium in the direction of the density decrease. Since we observe the steepening of the shock front the dust acoustic velocity must be decreasing with the dust density decrease. This is the condition required for the steepening of shocks in our case. The dust acoustic velocity is expressed as follows:

$$C_{da}=\sqrt{\frac{Z_d^2 T_i}{m_d}\frac{n_d}{n_i}}, \tag{1}$$

where Z_d is the dust particle charge, T_i is the ion temperature, m_d is the dust particle mass, and n_i and n_d are the ion and dust densities, respectively. As seen from Fig. 4 the dust density ahead of the front lies in the range $(0.5-2.5)\times 10^4$ cm^{-3}. The charge on the dust particle according to our measurements [15] is equal to $(1.5-3)\times 10^3$ e. The ion density is estimated to be in the range $(2-5)\times 10^8$ cm^{-3}. Therefore C_{da} ahead of the front varies between 0.4 and 3.1 cm/s. Taking into account the temporal variation of the dust density behind the shock front, $(5.2-7.0)\times 10^4$ cm^{-3}, we obtain $C_{da}=1.4-5.0$ cm/s. From these estimations we may conclude that the observed velocity of the shock front is of the order of the dust acoustic velocity, and the phenomenon we observe is of the dust-acoustic nature.

As we can see the shock is traveling in the medium with the decreasing dust density. However, in the high density region the dust density remains almost unchanged during the wave propagation. It means that the compression (ratio of the densities ahead of and behind the front) created by the shock

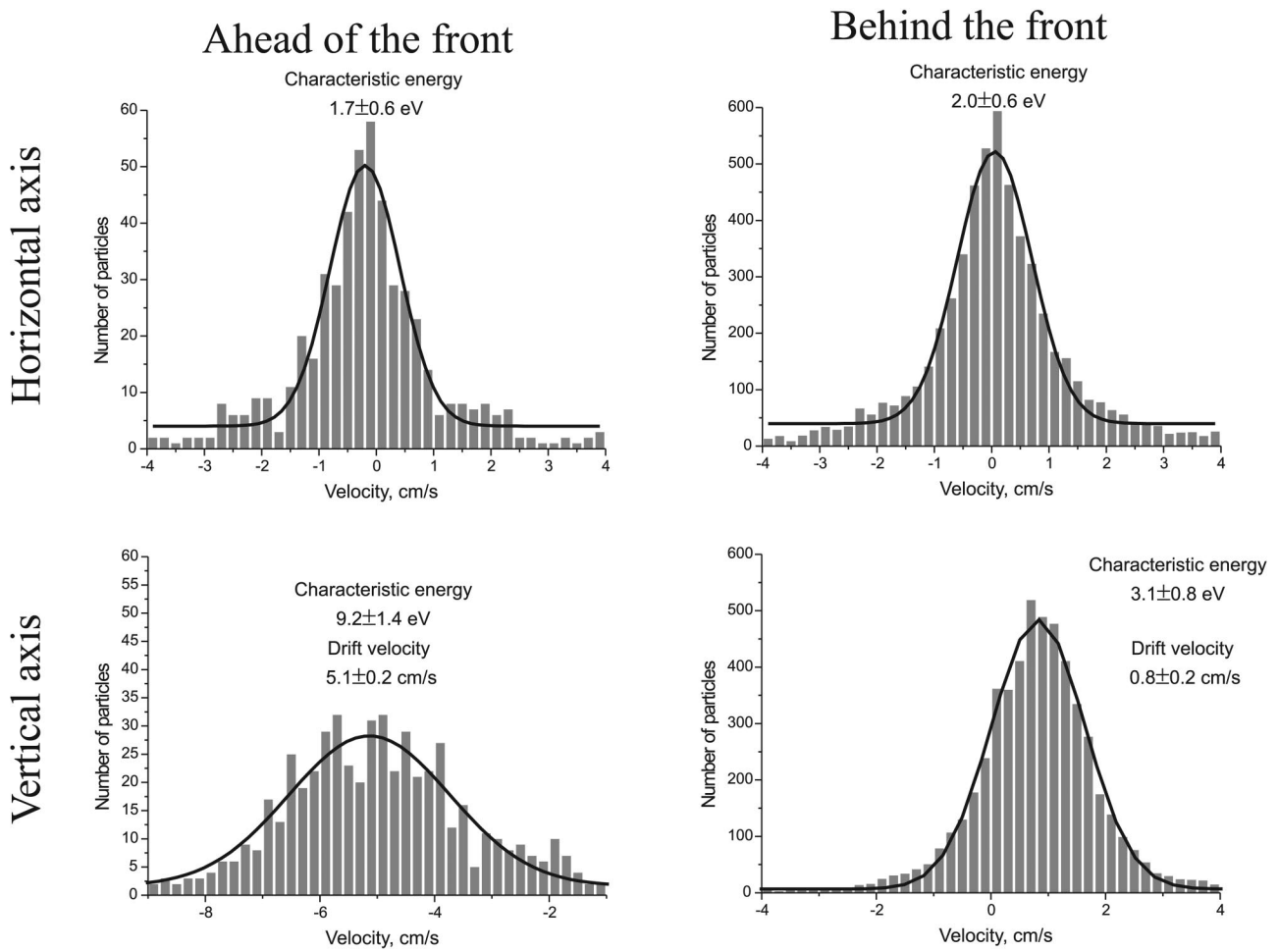

FIG. 6. Velocity distributions of the dust particles. Bars show the experimentally measured values and solid curves are the Gaussian fits. Characteristic energies are determined from the Gaussian fits as kinetic energies at which the number of the dust particles becomes *e* times smaller than in the maximum. Drift velocity corresponds to the maximum of the particle number.

is permanently increasing during the wave propagation and reaches the value of 15. This phenomenon was not observed in the previous shock experiment under microgravity conditions [9]. Such compression would be also abnormal for usual shocks known in gases or solids. Conservation laws limit the value of the shock compression to 10 [16].

The temperature of the dust component is much higher than that of the neutral gas. This anomalous heating is a well known phenomenon [17]. An unusual feature is the decrease of the average energy of the dust particles from the area ahead of the shock to the area behind the shock. This means that instead of the usual "shock heating," "shock cooling" is taking place.

The dusty plasma differs from the gaseous media in which the shock waves are traditionally being studied. The difference is not only in the fact that the charged dust grains interact with each other much stronger than the gas molecules, but also in that the external electric force and ion flow are present. Besides, the dust particles experience the drag force from the neutral molecules. In our previous works with the gas-dynamic excitation of the large amplitude waves [12] we have shown that these waves have an energy source other than the initial impulse. The present experiment is carried out at similar conditions and similar mechanisms seem to take place here. The wave must be gaining energy in the rarefaction zone. This energy gain may cause the abnormal compression and shock cooling we observe.

V. CONCLUSION

An electromagnetic impulse has been used to excite a perturbation in a dusty plasma structure. The perturbation had a character of discontinuity of the dust density and velocity. The steepening of the perturbation front was observed. So, we may conclude that the propagation of a compressive shock through the dusty plasma structure was observed. The shock compression in our experiment was reaching a very high value (up to 15) which is different from the shock characteristics in gases and solids in which the compression is limited to several times. Also the decrease of the average energy of the dust particles behind the shock front, i.e., shock cooling was observed. We suppose that energy transfer from the background plasma to the dust subsystem may be responsible for the phenomena of abnormal compression and shock cooling.

ACKNOWLEDGMENTS

The authors thank Dr. A. Starikovsky for helpful discussions. This work was supported by the Russian Foundation for Basic Research, Grant No. 03-02-16316 and the Presidium of the Russian Academy of Sciences, programme "Thermophysics and Mechanics of Extreme Power Impacts."

[1] H. K. Andersen, N. D'Angelo, and P. Michelsen, Phys. Fluids **11**, 606 (1968).
[2] R. J. Taylor, D. R. Baker, and H. Ikezi, Phys. Rev. Lett. **24**, 206 (1970).
[3] N. N. Rao, P. K. Shukla, and M. Y. Yu, Planet. Space Sci. **38**, 543 (1990).
[4] P. K. Shukla and A. A. Mamun, IEEE Trans. Plasma Sci. **29**, 221 (2001).
[5] F. Li and O. Havnes, Phys. Rev. E **64**, 066407 (2001).
[6] V. Nosenko, S. Nunomura, and J. Goree, Phys. Rev. Lett. **88**, 215002 (2002).
[7] D. Samsonov *et al.*, Phys. Rev. Lett. **83**, 3649 (1999).
[8] A. Melzer, S. Nunomura, D. Samsonov, Z. W. Ma, and J. Goree, Phys. Rev. E **62**, 4162 (2000).
[9] D. Samsonov *et al.*, Phys. Rev. E **67**, 036404 (2003).
[10] V. E. Fortov, A. G. Khrapak, S. A. Khrapak, V. I. Molotkov, A. P. Nefedov, O. F. Petrov, and V. M. Torchinsky, Phys. Plasmas **7**, 1374 (2000).
[11] http://www.ihed.ras.ru/nnapr/swform/index.shtml
[12] V. E. Fortov, O. F. Petrov, V. I. Molotkov, M. Y. Poustylnik, V. M. Torchinsky, A. G. Khrapak, and A. V. Chernyshev, Phys. Rev. E **69**, 016402 (2004).
[13] V. E. Fortov *et al.*, Phys. Lett. A **229**, 317 (1997).
[14] S. Nunomura, J. Goree, S. Hu, X. Wang, and A. Bhattacharjee, Phys. Rev. E **65**, 066402 (2002).
[15] V. E. Fortov, A. P. Nefedov, V. I. Molotkov, M. Y. Poustylnik, and V. M. Torchinsky, Phys. Rev. Lett. **87**, 205002 (2001).
[16] Ya. B Zeldovich and Yu. P. Raizer, *Physics of Shock Waves and High Temperature Hydrodynamic Phenomena* (Academic, New York, 1967).
[17] V. V. Zhakhovskii *et al.*, JETP Lett. **66**, 419 (1997).